Programmed Death-1 Antibody Blocks Therapeutic Effects of T-Regulatory Cells in Cockroach Antigen-Induced Allergic Asthma

Halvor S. McGee[1], Hideo Yagita[4], Zhifei Shao[1], and Devendra K. Agrawal[1,2,3]

Departments of [1]Biomedical Sciences, [2]Medicine, and [3]Medical Microbiology and Immunology, Center for Clinical and Translational Science, Creighton University School of Medicine, Omaha, Nebraska; and [4]Juntendo University School of Medicine, Tokyo, Japan

We recently reported that the adoptive transfer of T-regulatory cells (Tregs) isolated from lung and spleen tissue of green fluorescent protein–transgenic mice reversed airway hyperresponsiveness and airway inflammation. Because Programmed Death-1 (PD-1) is a pivotal receptor regulating effector T-cell activation by Tregs, we evaluated whether PD-1 is involved in the therapeutic effect of naturally occurring Tregs (NTregs) and inducible Tregs (iTregs) in cockroach (CRA)-sensitized and challenged mice. The $CD4^+CD25^+$ NTregs and $CD4^+CD25^-$ iTregs isolated from the lungs and spleens of BALB/c mice were adoptively transferred into CRA-sensitized and CRA-challenged mice with and without anti–PD-1 antibody (100 μg/mice). The $CD4^+CD25^+$ T cells in the lung were phenotyped after adoptive transfer. Concentrations of IL-4, IL-5, IL-10, IFN-γ, and IL-13 in bronchoalveolar lavage fluid (BALF) were measured using ELISA. The NTregs and iTregs from either lung or spleen tissue reversed airway hyperresponsiveness for at least 4 wk. However, the therapeutic effect was blocked by administering the anti–PD-1 antibody. The administration of Tregs-recipient mice with anti–PD-1 antibody significantly decreased cytotoxic T-lymphocyte antigen-4 expression, with low concentrations of Forkhead-winged transcriptional factor box 3 (Foxp3) mRNA transcripts in lung $CD4^+CD25^+$ T cells. These mice had substantially higher concentrations of BALF IL-4, IL-5, and IL-13, but significantly decreased levels of BALF IL-10. Adoptive therapy recipients without the anti–PD-1 antibody exhibited high levels of CTLA-4 expression and Foxp3 transcripts in lung $CD4^+CD25^+$ T cells, with a significant decrease in BALF IL-4, IL-5, and IL-13 concentrations and a substantial increase in BALF IL-10 concentrations. These data suggest that the reversal of airway hyperresponsiveness and airway inflammation by Tregs is mediated in part by PD-1, because other costimulatory molecules (e.g., inducible costimulatory molecule [ICOS] or CTLA-4) have been shown to play a role in Treg-mediated suppression.

Keywords: airway hyperresponsiveness; airway inflammation; anti–PD-1 antibody; cockroach antigen; Forkhead-winged transcriptional factor box P3

Asthma is a complex chronic inflammatory disease of the airways, characterized by repeated episodes of airway hyperresponsiveness (AHR) (1) and allergic airway inflammation (2). Uncontrolled asthma results in structural changes in the lung (3). Activated Th2 cells and the release of their signature cytokines, IL-4, IL-5, IL-9, and IL-13 (4), play a major role in the initiation and pathophysiology of asthma. Airway remodeling, a pathologic sequela of asthma, results from repeated exposure to Th2 cytokines. The $CD4^+CD25^+$ T-regulatory cells (Tregs) have been described in terms of their inherent capacity to regulate the immune response and prevent the development of a skewed Th1 and Th2 cell ratio in mice (5–7). The Tregs constitutively express CD25, the α chain of the IL-2 receptor complex. However, CD25 is also expressed on activated T cells during transient stages (8). Moreover, genetic anomalies of IL-2 or CD25 in humans and rodents result in the development of allergies, inflammatory bowel disease, and autoimmune diseases such as type 1 diabetes (9–11). To date, the best marker that specifically identifies Tregs is the Forkhead-winged transcriptional factor box 3 protein (Foxp3), which is critical for the development and function of Tregs (12–14). However, it is not expressed in all subsets of Tregs. In addition, a cumulative list of markers and cytokines was used to identify this specialized subset of T-lymphocytes; these may be found in some Treg populations, but not all. These include glucocorticoid-inducible tumor necrosis factor receptor (GITR), IL-10, lymphocyte activator gene 3 (LAG-3), transforming growth factor beta (TGF-β)/latency associated peptide (LAP-1), the inducible costimulatory molecule (ICOS), CD62L, B and T-lymphocyte attenuator (BTLA), CTLA-4, and recently, Programmed Death-1 (PD-1).

PD-1 is a 55-kD type I transmembrane protein of the immunoglobulin superfamily (15). It belongs to the CD28/CTLA-4 subfamily, and contains a single IgV-like domain in its extracellular region (16, 17). The PD-1 cytoplasmic region contains two tyrosine residues: (*1*) an immunoreceptor tyrosine-inhibitor motif (ITIM), and (*2*) an immunoreceptor tyrosine-based switch motif (ITSM) (18). The ITSM appears to be a principal factor in the modulation of T-cell activation (19), and PD-1 has a significant role in peripheral tolerance (20). There are two ligands for the PD-1 receptor: PD-L1 (B7-H1, CD274) and PD-L2 (B7-DC, CD273) (21). The ligand PD-1–PD-L1 belongs to the CD28-B7 signaling family, and this signaling pathway inhibits T-cell activity (15). The interaction of PD-L1 and PD-1 leads to cell-cycle arrest in the G0/G1 phase, but it does not increase cell death (21). In addition, PD-L2 has an affinity for PD-1 that is 2 to 6 times higher than that of PD-L1 (22, 23).

We recently reported that the adoptive transfer of GFP-labeled "naturally occurring" $CD4^+CD25^+$ T-regulatory cells

CLINICAL RELEVANCE

The expression and activity of PD-1 in T regulatory cells could provide a target to develop better therapeutic approaches to manage and control allergen-induced allergic airway inflammation and airway hyperresponsiveness in asthma.

(*Received in original form July 13, 2009 and in final form September 19, 2009*)

This study was supported by grant R01 HL070885 from the National Institutes of Health (to D.K.A.).

The contents of this report are solely the responsibility of the authors, and do not necessarily represent the official views of the National Heart, Lung, and Blood Institute or the National Institutes of Health.

Correspondence and requests for reprints should be addressed to Devendra K. Agrawal, Ph.D., M.B.A., Department of Biomedical Sciences, Creighton University School of Medicine, CRISS II, Room 510, 2500 California Plaza, Omaha, NE 68178. E-mail: dkagr@creighton.edu

Am J Respir Cell Mol Biol Vol 43. pp 432–442, 2010
Originally Published in Press as DOI: 10.1165/rcmb.2009-0258OC on November 9, 2009
Internet address: www.atsjournals.org

(NTregs) and "inducible" $CD4^+CD25^-$ T-regulatory cells (iTregs), isolated from the lung and spleen tissue of GFP-transgenic BALB/c mice, migrated to the lungs and lymph nodes of cockroach-sensitized and cockroach-challenged mice, and reversed AHR and airway inflammation (24). The $CD4^+CD25^-$iTregs, upon adoptive transfer, differentiated into $CD4^+CD25^+Foxp3^+$ in the lung of cockroach antigen (CRA)-sensitized and CRA-challenged mice, and these cells expressed substantially high concentrations of PD-1 (24).

In this study, we examined the role of PD-1 in the therapeutic effects of Tregs, and evaluated the effect of an anti–PD-1 antibody (aPD-1^{ab}) with an adoptive transfer of NTregs and iTregs derived from the lung and spleen tissue of naïve BALB/c mice into cockroach-sensitized and cockroach-challenged mice. We found that recipient mice of NTregs and iTregs from either lung or spleen tissue underwent a reversal of AHR and allergic airway inflammation, and the therapeutic effect lasted for at least 4 weeks. However, this effect was blocked by administering aPD-1^{ab}, suggesting that the PD-1 receptor is crucial for Tregs to modulate AHR and airway inflammation in allergic asthma.

MATERIALS AND METHODS

Mice

Four- to five-week-old BALB/c female mice were purchased from Harlan Laboratories (Indianapolis, IN), and were housed in separate cages according to our treatment protocol. Food and water were provided *ad libitum*. The research protocol of this study was approved by the Institutional Animal Care and Use Committee of Creighton University.

Induction of AHR by Sensitization and Challenge with CRA

A CRA-sensitized and CRA-challenged model of allergic airway inflammation was induced by two intraperitoneal injections of CRA antigen (10 μg), a mixture of (American) *Periplaneta Americana* (Linnaeus) and (German) *Blattella germanica* (Linnaeus) (Hollister Stier Laboratories, LLC, Spokane, WA), emulsified in imject alum (Pierce, Rockford, IL) in a total volume of 100 μl/mouse on Days 0 and 14. On Days 28–30 and Day 32, mice received an aerosol challenge of CRA antigen (50 mg/ml). On Day 33, AHR to methacholine was measured according to the established methods in our laboratory (24, 25) (Figure 1).

Assessment of Specific Airway Resistance

To confirm AHR to methacholine, several randomly selected sensitized and sham-treated mice were anesthetized, cannulated, and tracheostomized. Mice were placed in supine position, with the attached cannula connected to the port in the single-chamber plethysmograph for anesthetized animals model number PLY3111 (Buxco Electronics, Wilmington, NC). Mice were mechanically ventilated with Harvard Rodent Ventilator model 683 (Harvard Apparatus, Holliston, MA). Mice were challenged with aerosolized PBS, followed by increasing doses of methacholine (3.1, 6.25, 12.5, 25, 50, and 100 mg/ml) to measure specific airway resistance (24, 25).

Isolation of T-Regulatory Cells for Adoptive Transfer

We isolated $CD4^+CD25^+$ and $CD4^+CD25^-$ from the lungs and spleens of BALB/c mice by the method previously reported (24, 25). Briefly, tissues were digested using collagenase D (Roche Molecular Systems, Pleasanton, CA) (1 mg/ml) and 5 ml of RPMI-1640 (Cambrex, East Rutherford, NJ), and incubated at 37°C in a CO_2 incubator for 90 min. Red blood cells were lysed using Tris-buffered ammonium chloride solution, and the suspension was neutralized with sterile PBS solution containing 4% FBS. The suspension was centrifuged at 350 × *g* for 10 min. The supernatant was discarded, and the pellet was washed in 10 ml of Hanks' Balanced Buffered Solution, centrifuged, and resuspended in an AutoMACS (Miltenyi Biotec, Auburn, CA) running buffer. This was followed by isolating Tregs, using a two-step process. The $CD4^+$ T cells were pre-enriched by depleting unwanted cells, using a cocktail of antibodies. Then $CD25^+$ cells were positively selected from the enriched $CD4^+$ T-cell fraction ($CD4^+$ $CD25^+$ T-Regulatory Cell Isolation Kit; Miltenyi Biotec, Auburn, CA). The remaining $CD4^+$ cells were designated as $CD4^+CD25^-$ cells. The purity of $CD4^+CD25^+$ cells from lung tissue was 75–78%, and the purity of $CD4^+CD25^+$ cells from spleen tissue was 93–97%. The purity of the $CD4^+CD25^-$ donor-cell population from lung tissue (97%) was comparable to that in the cells from spleen tissue (98%) (24).

Adoptive Transfer of $CD4^+CD25^+$ and $CD4^+CD25^-$ T Cells and the Administration of aPD-1^{ab} in Cockroach-Sensitized and Cockroach-Challenged Mice

Cockroach-sensitized and cockroach-challenged mice were randomized into eight groups to receive an adoptive transfer of 400,000 cells/mouse in 50 μl of sterile PBS with or without PD-1 antibody (100 μg/mouse): (1) the lung NTregs ($L25^+$) groups received lung NTregs with and without aPD-1^{ab}, (2) the lung iTregs ($L25^-$) groups received lung iTregs with and without aPD-1^{ab}, (3) the spleen NTregs ($S25^+$) groups received spleen NTregs with and without aPD-1^{ab}, and (4) the spleen iTregs ($S25^-$) groups received spleen iTregs and without aPD-1^{ab}. Cells were injected intravenously into the tail vein, followed by an intraperitoneal injection of CRA antigen to prime the injected cells. The next 4 wk before each 3-d aerosol challenge, mice received aPD-1^{ab}, and AHR to methacholine was evaluated at the end of each week (Figure 1).

FACS Analysis and Antibodies

Freshly isolated $CD4^+CD25^+$ T cells were isolated and examined for surface molecule expression, using a FACScan (BD Biosciences, San Jose, CA) flow cytometer, and data were processed with CellQuest Pro (BD Biosciences), using our established standard protocol for cell preparation. The following monoclonal antibodies (mAbs), conjugated to fluorochromes, were used: CD4-PerCP (clone L3T4), CD69-FITC (clone H12F3), CD62L-FITC (clone MEL-14), CTLA-4-FITC (UC10–4F10–11) were purchased from BD Bioscience. We purchased CD25-PE (clone 4E3) from Miltenyi Biotec). We purchased GITR-PerCP (clone DTA-1), ICOS-APC (clone 7e.17G9), and PD1-FITC (clone J43) antibodies from E-Bioscience (San Diego, CA). Anti–PD-1 antibody (RMP1–14) was provided by Dr. Hideo Yagita (Juntendo University School of Medicine, Tokyo, Japan). The anti-mouse PD-1 mAb (hybridoma RMP1–14, rat IgG2a) was produced against mouse PD-1 transfectant. This anti-mouse PD-1 mAb blocks the binding of both PD-L1-Ig and PD-L2-Ig to the PD-1 receptor transfectants, just like the J43 clone of PD-1 (26, 27). Each mouse received 100 μg of PD-1 mAb via the dorsal tail vein. No adverse effects were evident in any mouse.

Characterization of NTregs and iTregs Before and After Adoptive Transfer

Naturally occurring Tregs and iTregs before adoptive transfer were characterized on the basis of phenotype by the following expression: $L25^+$ donor cells were $ICOS^-$, $CD62L^+$, $GITR^+$, $PD\text{-}1^-$, $CD69^-$, and $CD25^+$. The $L25^-$ donor cells had the same phenotype, with the exception of being $CD25^-$. The $S25^+$ donor cells expressed low levels of ICOS, $CD69^-$, CD62L, $PD\text{-}1^-$, $GITR^+$, and $CD25^+$. Similarly, $S25^-$ donor cells were the same, with the exception of being $CD25^-$, as we recently reported (24). In addition, mRNA isolated from $CD4^+CD25^-$ and $CD4^+CD25^+$ T cells before adoptive transfer was examined for the expression of Foxp3 (24). The adoptively transferred $CD4^+CD25^-$ T cells were $Foxp3^-$, and $CD4^+CD25^+$ T cells were $Foxp3^+$. Subsequently, the Tregs isolated from the lungs of cockroach-sensitized and cockroach-challenged mice after adoptive transfer were $CD4^+CD25^+Foxp3^+$ $PD\text{-}1^+CTLA\text{-}4^+$ Tregs.

BALF and Cytokine Analysis

Mice were anesthetized with sodium pentobarbital. Lungs were gently lavaged with 1 ml of warm saline solution (37°C) via a tracheal cannula. A Coulter counter (Beckman and Coulter, San Diego, CA) was used to count total numbers of cells. All samples were centrifuged at 1,500 rpm

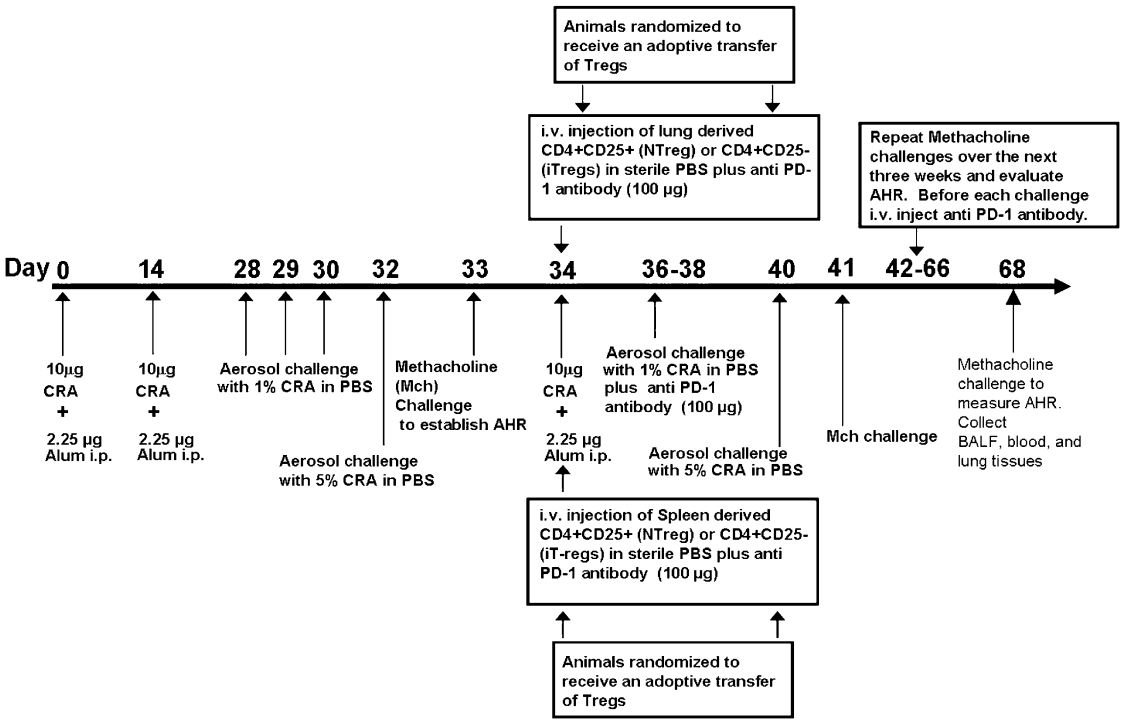

Figure 1. Protocol to sensitize BALB/c mice with cockroach antigen (CRA), adoptive transfer of T regulatory cells (Tregs), and the administration of anti–PD-1 antibody (aPD-1^{ab}). Mice on Days 0 and 14 received an intraperitoneal injection of CRA antigen. Mice on Days 28–30 and 32 were aerosol-challenged with CRA antigen. On Day 33, airway hyperresponsiveness (AHR) to methacholine was established. For adoptive transfer treatment, on Day 33, animals were randomized and received an adoptive transfer of Tregs plus anti–PD-1 antibody. On Day 34, mice received another intraperitoneal injection of CRA antigen. In the anti–PD-1 therapy phase, aPD-1^{ab} is given each week before each 3-day aerosol challenge. In addition, mice received a rigorous 4 weeks of CRA antigen challenge, and at the end of each week, AHR to methacholine was evaluated. On Day 68, the mice were killed for analysis.

for 10 min, and the supernatant was stored at −80°C until ELISA was performed. The levels of IFN-γ, IL-4, IL-5, IL-10, and IL-13 in bronchoalveolar lavage fluid (BALF) were measured using Th1/Th2, IL-5, and IL-13 ELISA Detection Ready-Set-Go Kits (E-Bioscience), according to the manufacturer's protocol.

Fixation of Lung Tissue and Morphometric Analysis

Lungs were removed, and a section of the left lobe was placed in 4% formalin. The formalin was removed, and tissue was placed in 70% ethanol and embedded in paraffin, using a Sakura Tissue-Tek VIP paraffin processor (IMEB, San Marcos, CA). Thin sections were cut (5 μm) and stained with hematoxylin and eosin and trichrome stain, using a Masson trichrome staining kit (IMEB). Five separate areas in the stained histologic slides were randomly selected from representative airways in the lung tissue for quantitative analyses of lumen-to-wall ratio, height of epithelial cells from the base to the top of cells, and size of the smooth muscle cell layer, using DP Controller Imaging Software (Olympus America, Inc., Central Valley, PA).

RT-PCR

The cell pellet from the sorted $CD4^+CD25^+$ T cells from the lungs of cockroach-sensitized and cockroach-challenged mice after adoptive transfer was placed in 1 ml of Trizol Reagent, and incubated for 15 min at room temperature. We added 1-bromo-3-chloropropane (100 μl) to each Eppendorf tube containing cells, and each Eppendorf tube was vigorously shaken for approximately 5 seconds and incubated for 15 minutes at room temperature. The cell lysate was centrifuged at 12,000 × *g* for 15 minutes at 4°C. The aqueous phase (top clear layer) was transferred into a new tube, and 500 μl of isopropanol were added, mixed, and incubated for 5 to 10 minutes at room temperature, and then centrifuged at 12,000 × *g* for 8 minutes at 4°C. The RNA pellet was mixed with 1 ml of 70% ethanol and centrifuged at 7,500 × *g* for 5 minutes at 4°C (Molecular Research Center, Inc., Cincinnati, OH). The RNA pellet was air-dried for 2 to 4 minutes and dissolved in 20 to 50 μl RNase-free water. The RNA samples (2 μl) were diluted in water (98 μl), and the concentration was quantified using a GeneQuant 1300 spectrophotometer (GE Healthcare Bio-Sciences Corp., Piscataway, NJ).

The ImProm-11 Reverse Transcription System (catalogue number A3800) was purchased from Promega (Madison, WI), and we followed the manufacturer's instructions. Experimental RNA (up to 1 μg/reaction) (3.0 μl), Oligo (dt) (1 μl), and nuclease-free water (1.0 μl) were combined in Eppendorf tubes. Each tube was placed into a preheated 70°C block for 5 minutes, and chilled in ice water for 5 minutes. Each tube was centrifuged to collect the condensate and maintained at the original volume of 5 μl. Then, 5× reaction buffer (4 μl), $MgCl_2$ 2.5 mM (3.2 μl), dNTP mix (0.5 mM), recombinant RNasin RNase inhibitor (0.5 μl), ImProm-II reverse transcriptase (1.0 μl), and nuclease-free water (5.3 μl) were used for the reverse-transcription reaction mixture, which was placed on the hot plate at 25°C for 5 minutes, 42°C for 60 minutes, 70°C for 15 minutes, and 4°C for 5 minutes.

Each PCR reaction mixture contained the PCR Master Mix (Promega) (25 μl), cDNA (2 μl), forward primer (5 μl and 1 μM), reverse primer (5 μl and 1 μM), and RNase/DNase-free water (13 μl). The PCR reaction mixtures were placed in the PCR machine heat block, and the cDNA was initially denatured at 95°C for 15 minutes. The PCR amplification was performed by denaturation for 60 seconds at 94°C, annealing for 60 seconds at 55°C, primer extension for 60 s at 72°C, and a final extension for 10 minutes at 72°C. Hypoxanthine-guanine phosphoribosyltransferase (HPRT) was used as an internal control. The Gene Amp PCR System 2400 (Perkin Elmer, Waltham, MS) was used at 32 cycles for Foxp3, and 28 cycles for HPRT. The forward primer for Foxp3 is 5′- TACACCCAGGAAAGAC AGCAACCT-3′ and the reverse primer is 5′-TCTGGAGTAGGC GAACATGCGAGT-3′. In addition, the forward primer for HPRT is 5′ - GATACAGGCCAGACTTTGTTG-3′ and the reverse primer is 5′-GGTAGGCTAGCCTATAGGCT-3′. Both Foxp3 and HPRT have a melting temperature of 50°C.

The PCR product was loaded onto a 1.5% agarose gel. After electrophoresis, the gels were photographed under ultraviolet light, using the UVP Bioimaging System (UVP, Upland, CA). Each experiment was performed three times. A densitometric analysis was performed to calculate the ratio of mRNA intensity of Foxp3 and the intensity of the housekeeping gene *HPRT*.

Data Analysis

Data were analyzed using GraphPad Prism (San Diego, CA) statistical analysis and graphing software. An unpaired Student *t* test was used to

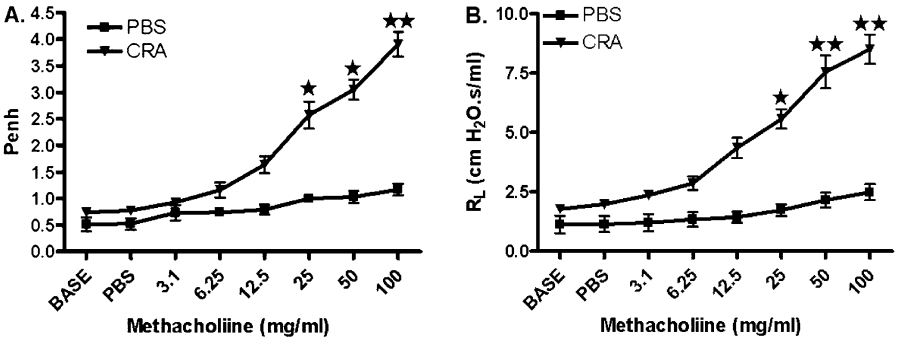

Figure 2. Airway hyperresponsiveness to methacholine. (*A*) On Day 33, AHR to methacholine (Mch) was established using a noninvasive, unrestrained, whole-body plethysmograph. (*B*) Airway hyperresponsiveness was validated by invasive tracheostomy and by measuring specific airway resistance (R_L) to Mch. Data are shown as mean ± SEM for five mice in each group. *$P < 0.01$. **$P < 0.001$.

determine statistical differences between the two groups according to Microsoft Excel (Microsoft Corp., Bethesda, MD). Multiple group comparisons were performed using ANOVA. $P < 0.05$ was considered significant.

RESULTS

Established AHR in CRA-Sensitized and CRA-Challenged Mice

Following the protocol shown in Figure 1, CRA-sensitized and CRA-challenged mice exhibited AHR to methacholine, which was examined with a noninvasive whole-body plethysmograph and confirmed with a more rigorous invasive method, involving tracheostomies to measure specific airway resistance. The administration of 100 mg/ml methacholine exhibited enhanced pause (Penh) values of 4.29 ± 0.26 (CRA group) and 1.0 ± 0.12 (PBS group) (Figure 2A). The specific airway resistance induced by 100 mg/ml methacholine exhibited mean values of 9.04 ± 2.63 $cmH_2O \cdot s/ml$ (CRA group) and 2.34 ± 0.23 $cmH_2O \cdot s/ml$ (PBS group) (Figure 2B).

Effect of aPD-1^{ab} on AHR in CRA-Sensitized and CRA-Challenged Mice

Mice in all groups that received an adoptive transfer of either NTregs or iTregs from lung or spleen tissue without aPD-1^{ab} exhibited a reversal of AHR. However, this effect was blocked with the administration of aPD-1^{ab}, and the AHR was comparable to the level in CRA-sensitized mice without adoptive transfer (CRA^{AT-}) (Figure 3). In addition, we examined the effect of an adoptive transfer of Tregs in normal control mice (PBS^{AT+}), and found that AHR or airway inflammation was not affected (Figure 3). Furthermore, control PBS mice that received aPD-1^{ab} showed significantly increased AHR to methacholine after wk 3 of methacholine challenge (Figure 3).

Effect of aPD-1^{ab} on the Histology of the Airways After Adoptive Transfer

Histologic results of all recipients of an adoptive transfer of Tregs plus aPD-1^{ab} exhibited severe inflammatory cell infiltration, hypertrophic epithelial cells, hyperplastic smooth muscle cells (Figure 4A), and collagen deposition, as indicated by blue staining (Figure 4B). These morphologic changes were comparable to those in CRA^{AT-} mice. Conversely, the lung histology in all recipient mice with adoptive transfer therapy without aPD-1^{ab} was nearly restored to the sham-sensitized level. In addition, nonsensitized mice that received adoptive transfer therapy exhibited no inflammatory changes, and were comparable to the PBS control mice (Figures 4A and 4B). Furthermore, control

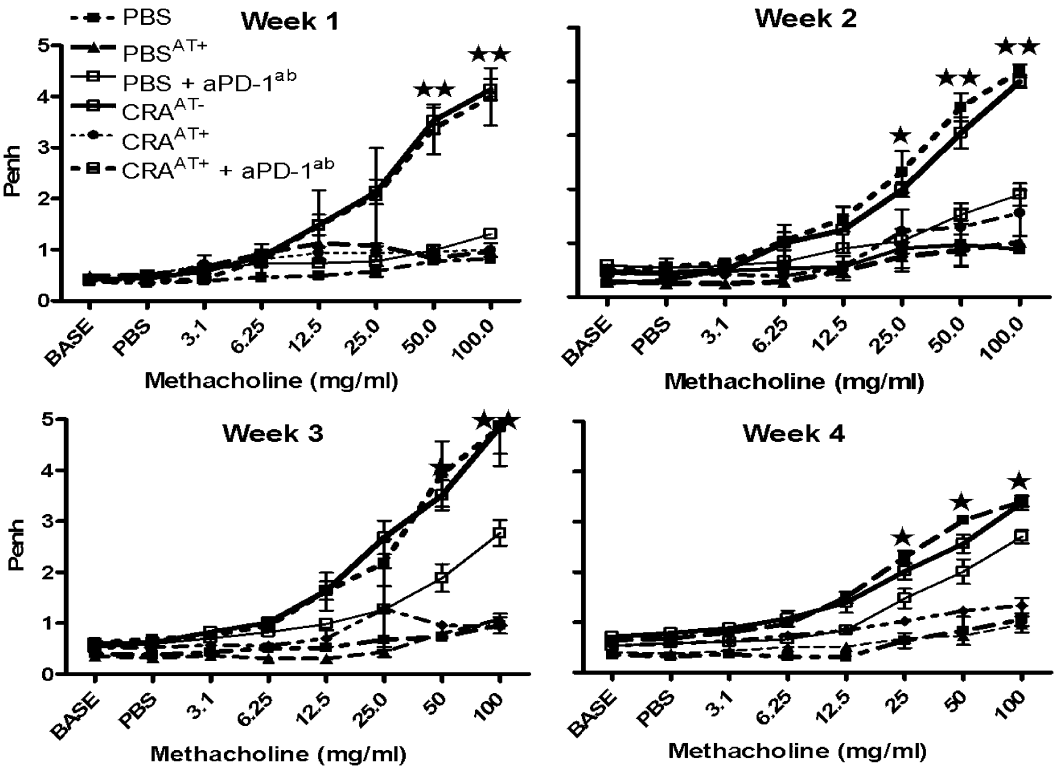

Figure 3. Pulmonary function after adoptive transfer and aPD-1 therapy. On Day 33, AHR was established, and on Day 34, mice received an adoptive transfer of NTregs and iTregs (400,000 cells/mouse) by intravenous injection with and without anti–PD-1 antibody (aPD-1^{ab}). Mice were aerosol-challenged for 4 wk, and at the end of each week, AHR was evaluated. These data are for the recipient mice of L25^{+} cells. However, we found that the data were very similar in all experimental groups. Therefore, this depiction is representative for each experimental group. The data in enhanced pause (Penh) values are presented as means ± SEM of five mice per group. *$P < 0.01$. **$P < 0.001$.

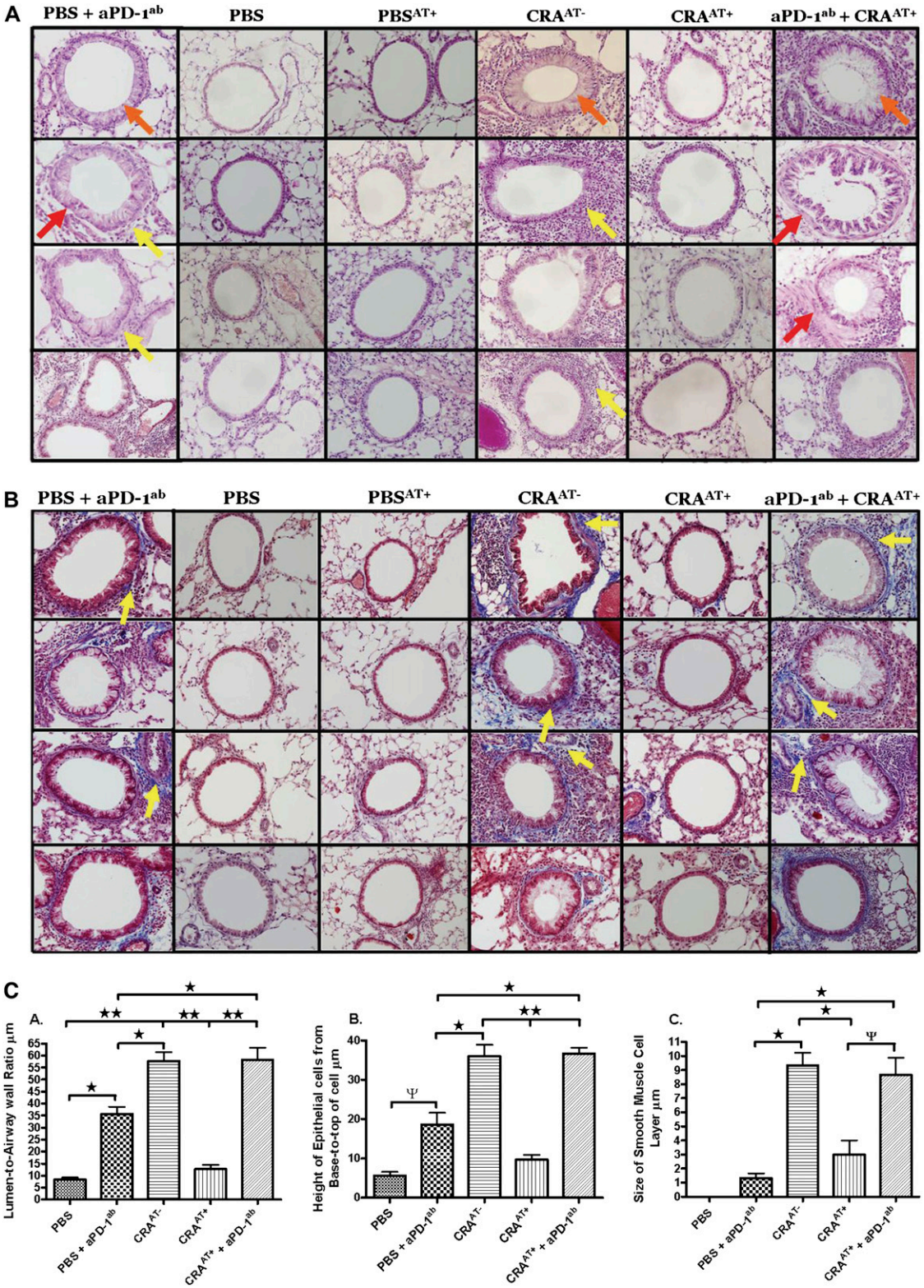

Figure 4. Lung histology after adoptive transfer. (*A*) Lung sections obtained after 4 wk of cockroach aerosol challenges from each treatment group. Sections were stained with hematoxylin and eosin, and morphology was examined by light microscopy. *Yellow arrows* indicate inflammatory cell infiltration surrounding the airways. *Orange arrows* indicate hypertrophy of airway epithelial cells. *Red arrows* indicate smooth muscle cell hyperplasia and hypertrophy. (*B*) Lungs were removed, embedded with paraffin, and sectioned (5 μm) after 4 wk of cockroach aerosol and methacholine challenges from each treatment group after adoptive transfer. Sections were processed by trichrome staining and evaluated for collagen deposition by light microscopy, as indicated by *yellow arrows*. These data are representative of five mice per group. (*C*) These datasets provide a comparative analysis of each experimental group, quantifying morphometric changes in the airways of normal-to-induced asthmatic mice and treated mice. The morphometric parameters include (*A*) lumen-to-airway wall ratio, (*B*) epithelial cell height, and (*C*) changes in thickness of smooth muscle cell layer.

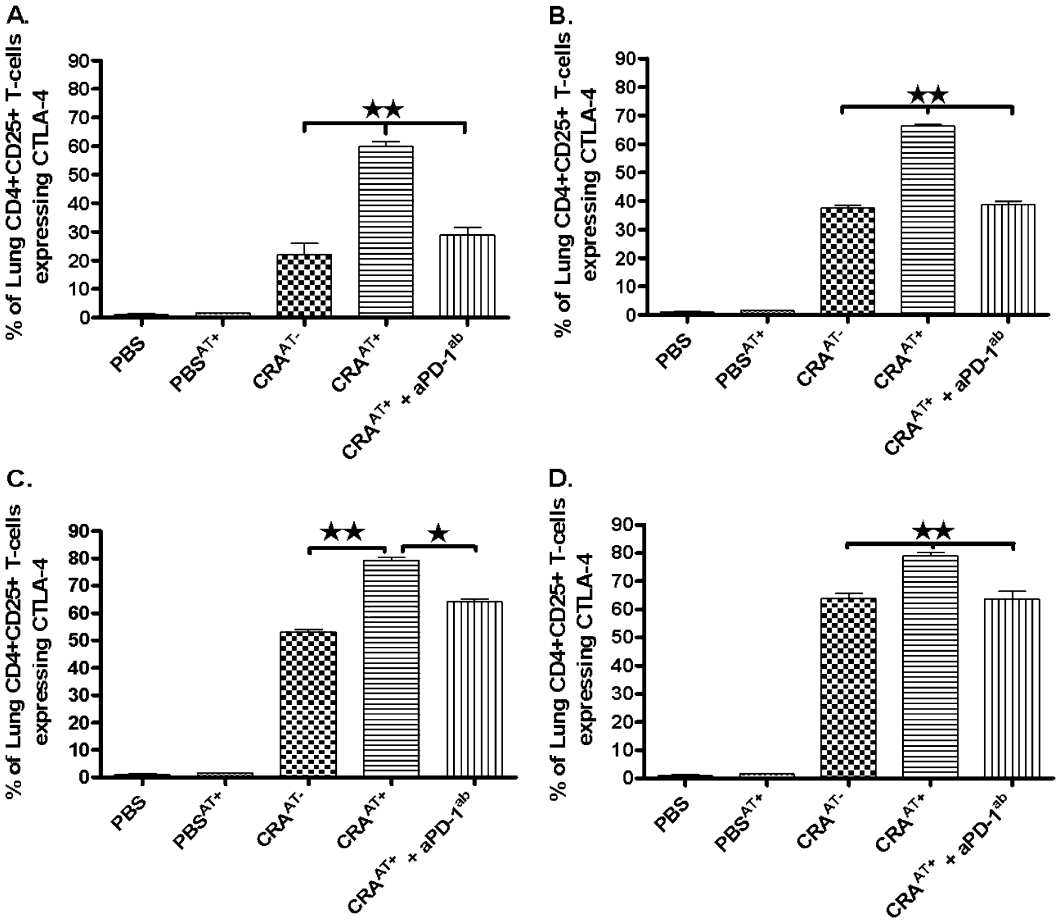

Figure 5. Expression of CTLA-4 in lung $CD4^+CD25^+$ T cells after adoptive transfer. The expression of CTLA-4 was examined in lung $CD4^+CD25^+$ T cells isolated from various experimental groups including PBS, PBS^{AT+}, CRA^{AT-}, CRA^{AT+}, and CRA^{AT+} plus aPD-1^{ab}. In these experiments, cells from either lung (*A*, $L25^+$; *B*, $L25^-$) or spleen (*C*, $S25^+$; *D*, $S25^-$) were adoptively transferred. The $CD4^+CD25^+$ T cells isolated from the lungs of all CRA^{AT-} mice showed a significant decrease in CTLA-4 expression, and this was similar to CTLA-4 expression in lung $CD4^+CD25^+$ T cells of mice treated with aPD-1^{ab}. However, CTLA-4 expression in lung $CD4^+CD25^+$ cells was significantly increased in mice that received the adoptive transfer. The expression of CTLA-4 in lung $CD4^+CD25^+$ cells was nominal-to-absent in PBS control mice and PBS mice with adoptive transfer. The data are presented as mean ± SEM of five mice per group. $*P < 0.01$, $**P < 0.001$.

PBS mice administered with aPD-1^{ab} exhibited significant inflammatory cell infiltration in the lung, with epithelial cell hypertrophy and a moderate level of collagen deposition (Figures 4A and 4B). There were no apparent differences in the adoptive transfer of Tregs between the two cell types of either tissue.

In cockroach-sensitized and cockroach-challenged mice without adoptive transfer (CRA^{AT-}) and cockroach-sensitized and cockroach-challenged mice with adoptive transfer plus aPD-1^{ab} (CRA^{AT+} + aPD-1^{ab}), the lumen-to-airway wall ratio, the epithelial cell height, and the thickness of the smooth muscle cell layer were substantially increased compared with cockroach-sensitized and cockroach-challenged mice with adoptive transfer (CRA^{AT+}), PBS + aPD-1^{ab}, and PBS (Figure 4C). This finding suggests a significant narrowing in the airways after challenge with aerosolized cockroach antigen, and this narrowing was attenuated by adoptive transfer. However, the administration of PD-1 antibody reversed the attenuated effect of adoptively transferred Tregs on morphometric changes in the airways (Figure 4C). This finding is supported by elevated AHR, as shown in Figure 3.

Expression of CTLA-4 in $CD4^+CD25^+$ T Cells Isolated from Lungs of Recipient Mice after Adoptive Transfer

The expression of CTLA-4 was examined in lung $CD4^+CD25^+$ T cells isolated from various experimental groups, including PBS, PBS^{AT+}, CRA^{AT-}, CRA^{AT+}, and CRA^{AT+} + aPD-1^{ab}. In these experiments, cells from either lung (Figure 5A, $L25^+$; Figure 5B $L25^-$) or spleen (Figure 5C, $S25^+$; Figure 5D, $S25^-$) were adoptively transferred. The lung $CD4^+CD25^+$ T cells from mice that received the adoptive transfer plus aPD-1^{ab} displayed a substantial reduction in CTLA-4 expression, compared with a significant increase in cells from mice without aPD-1^{ab}. The decreased expression of CTLA-4 in $CD4^+CD25^+$ T cells from mice that received aPD-1^{ab} paralleled that in CRA-sensitized mice without adoptive transfer. The $CD4^+CD25^+$ T cells in the PBS control and PBS^{AT+} mice showed nominal-to-absent expression of CTLA-4 (Figure 5). The pattern in CTLA-4 expression in $CD4^+CD25^+$ Tregs in various experimental groups was similar, irrespective of the $CD25^-$ or $CD25^+$ phenotype of adoptively transferred cells from spleen or lung tissue (Figure 5).

Effect of aPD-1^{ab} plus Adoptive Transfer on Leukocytes in BALF

The aPD-1^{ab} significantly blocked the beneficial effect of the adoptive transfer of Tregs in all groups of mice, and significantly increased BALF eosinophils and lymphocytes, mimicking the results in CRA^{AT-} mice (Figures 6A–6D).

Expression of Foxp3 Transcripts from $CD4^+CD25^+$ T Cells Isolated from Lungs of Mice with and without aPD-1^{ab} plus Adoptive Transfer Tregs

The expression of Foxp3 mRNA was significantly increased in $CD4^+CD25^+$ T cells isolated from the lungs of all mice that received an adoptive transfer of either NTregs and iTregs from lung and spleen tissue without aPD-1^{ab} treatment (Figure 7, *lane 4*). However, the expression of Foxp3 transcripts was substantially reduced in $CD4^+CD25^+$ T cells isolated from the lungs of all mice that received the adoptive transfer plus aPD-1^{ab} of either NTregs and iTregs from spleen or lung tissue (Figure 7, *lane 5*). Conversely, $CD4^+CD25^+$ T cells isolated from the lungs of cockroach-sensitized and cockroach-challenged

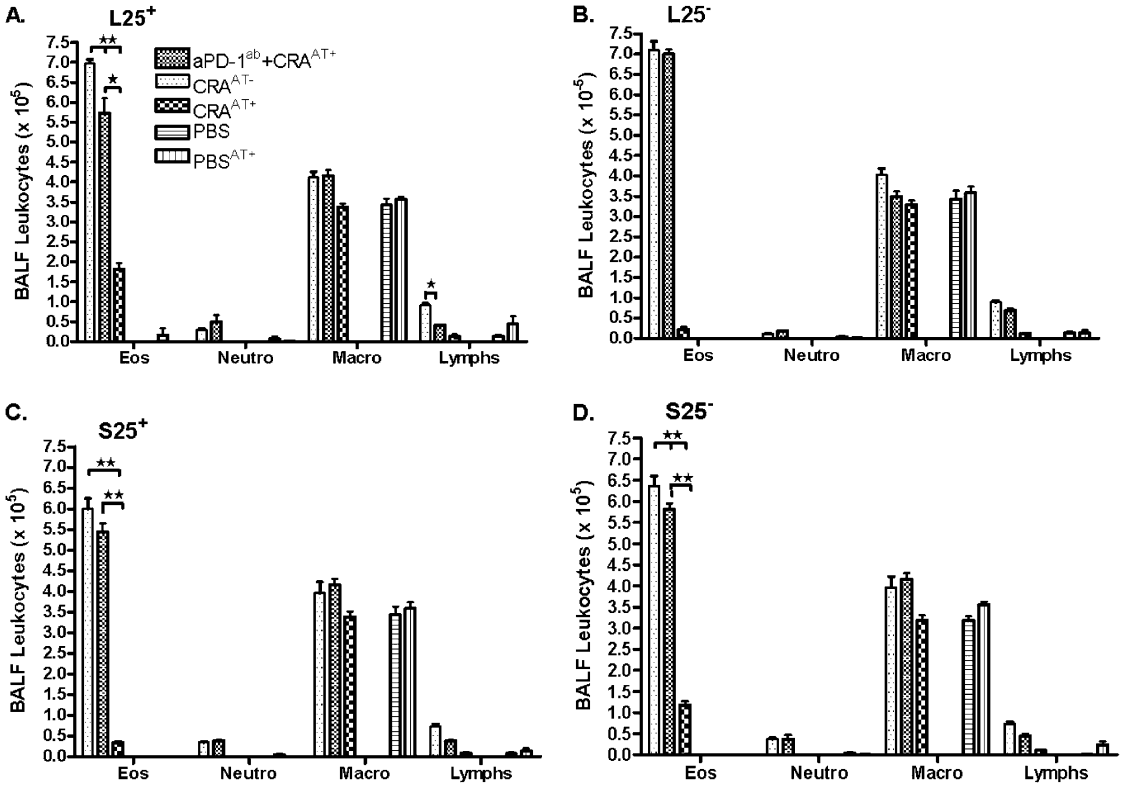

Figure 6. Leukocytes in BALF after adoptive transfer. Eosinophils in the BALF of all CRA^{AT-} mice were significantly increased after cockroach sensitization. This effect was paralleled in all mice that received aPD-1^{ab}. However, the adoptive transfer of Tregs significantly decreased the density of eosinophils to the PBS control level. No adverse effects were seen in the BALF of PBS mice that received adoptive transfer. The data are presented as mean ± SEM of five mice per group. $*P < 0.01$, $**P < 0.001$.

mice without an adoptive transfer or aPD-1^{ab} exhibited very low but detectable levels of Foxp3 transcripts (Figure 7, *lane 3*). In contrast, Foxp3 was constitutively expressed in both PBS control mice and PBS mice with adoptive transfer (PBS^{AT+}) (Figure 7, *lanes 1* and *2*).

Cytokine Concentrations in BALF

In all groups that received the adoptive transfer of either NTregs or iTregs from lung or spleen tissue, a significant reduction occurred in IL-4, IL-5, and IL-13 concentrations in BALF (Table 1). Such a reduction in Th2 cytokines was blocked after the administration of aPD-1^{ab} with an adoptive transfer of NTregs or iTregs from lung or spleen tissue, comparable to the cockroach-sensitized and cockroach-challenged mice without adoptive transfer (Table 1). The PBS^{AT+} mice exhibited no adverse effects of the adoptive therapy. The adoptive transfer of NTregs or iTregs of either tissue caused a significant increase in concentration of BALF IL-10, which was inhibited by the administration of PD-1^{ab} (Table 1). In addition, we examined concentrations of IFN-γ, a Th1 cell cytokine in BALF. Cockroach-sensitized and cockroach-challenged mice with adoptive transfer in all experimental groups exhibited a significant increase in BALF IFN-γ concentrations, compared with cockroach-sensitized and cockroach-challenged mice without adoptive transfer, and cockroach-sensitized and cockroach-challenged mice with adoptive transfer plus aPD-1^{ab}. These data suggest that IFN-γ could be secreted from Th1 cells and/or possibly Tregs. Akbari and colleagues (2) reported the development of a Th1-like Treg that secreted large amounts of IFN-γ in response to antigen challenge (Figure 8).

DISCUSSION

In this report, we found that the adoptive transfer of Tregs induced a significant reduction in AHR, inflammatory leukocytes in BALF, and proinflammatory cytokine, IL-4, IL-5, and IL-13, levels of the BALF, but significantly increased concentrations of BALF IL-10. However, this therapeutic effect was blocked by the administration of aPD-1^{ab}. The PD-1 antibody caused a significant increase in eosinophils, lymphocytes, IL-4, IL-5, and IL-13 in the BALF, but with a significant decrease in BALF IL-10 concentrations. These data suggest a pivotal role of PD-1 in the modulation of AHR and airway inflammation in our murine model of cockroach-induced allergic asthma. The elevated pulmonary data of cockroach-sensitized and cockroach-challenged mice without adoptive transfer and with adoptive transfer plus anti–PD-1 antibody correlated well with the histology. As indicated by the histology, perivascular and peribronchial inflammatory cell infiltration (*yellow arrow*), epithelial cell hypertrophy and damage (*orange arrows*), airway smooth muscle thickening, and collagen deposition were evident. However, cockroach-sensitized and cockroach-challenged mice with adoptive transfer exhibited a reversal of airway inflammation, and changes in histology nearly paralleled those in PBS control mice. In addition, AHR did not increase in PBS mice treated with aPD-1^{ab} until Week 3 and Week 4 in response to treatment with PBS. During the first 2 weeks of challenge with PBS, AHR was normal, which may represent a normal response in healthy animals. However, the moderate increase in AHR that was observed in mice during the later challenges of Week 3 and Week 4 may be attributable to the inability of the ligands (PD-L1 and PD-L2) to bind to the PD-1 receptor on Tregs for immune response. These results seen in the PBS + aPD-1^{ab} mice are similar to those in PD-1 knockout mice. Nishimura and colleagues (28) demonstrated that PD-1 knockout mice grew normally, compared with normal mice. However, over a period of time, the histology of these mice showed severe splenomegaly and a significant increase in T-cell and B-cell cellularity. However, cockroach-sensitized and cockroach-challenged mice without adoptive transfer and with adoptive

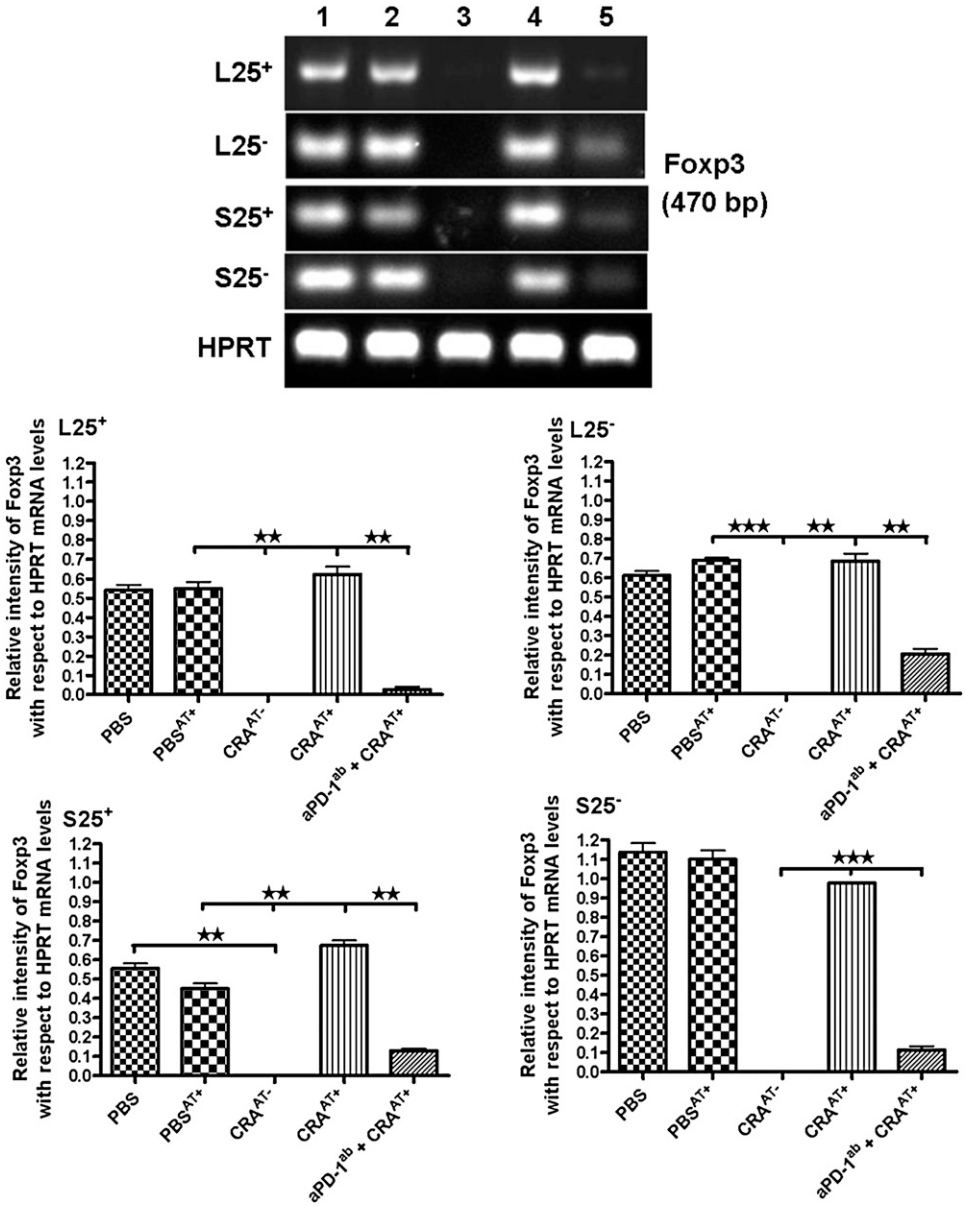

Figure 7. Expression of Foxp3 (470 bp) in lung CD4$^+$CD25$^+$ T cells after adoptive transfer. The expression of Foxp3 in lung CD4$^+$CD25$^+$ T cells was very low, but was detectable after cockroach sensitization. A similarly low expression of Foxp3 in lung CD4$^+$CD25$^+$ T cells was observed after administration of aPD-1^{ab}. However, an adoptive transfer of Tregs completely restored Foxp3 expression in lung CD4$^+$CD25$^+$ T cells. Densitometric analyses confirmed the PCR data, as shown by the ratio of the intensity of Foxp3 mRNA and HPRT. *$P < 0.01$, **$P < 0.001$, ***$P < 0.0001$.

transfer plus aPD-1^{ab} exhibited a substantial increase in AHR and airway inflammation over the same period of time, compared with PBS plus aPD-1^{ab} mice. These data suggest that the reversal of antigen-induced AHR and airway inflammation in mice is modulated by Tregs, using a PD-1/PD-L1 and/or PD-L2 axis signaling pathway. Polanczyk and colleagues (29) demonstrated that Tregs isolated from PD-1 knockout mice were deficient at suppressing effector T cells *in vitro*. But when these Tregs were treated with an immunomodulatory estrogen (17-β-estradiol), their functional capacity was partially restored and enhanced the expression of PD-1 expression. Thus, these reports support our conclusion that Tregs use the PD-1 receptor to suppress effector T cells, and the therapeutic effect of adoptively transferred Tregs was blocked by the anti–PD-1 antibody. However, the signaling pathway of PD-1 and Tregs is ill-defined and certainly warrants further investigation.

The CD4$^+$CD25$^+$ T cells purified from the lungs of all mice that received the adoptive transfer of either NTregs or iTregs of either tissue plus aPD-1^{ab} showed a significant reduction of CTLA-4 expression, suggesting that CTLA-4 may work in concert with PD-1 and/or may use a different pathway to reverse AHR and airway inflammation. Parry and colleagues (30) showed that PD-1 and CTLA-4 are both necessary for T-cell inhibition, although their inhibition signaling pathways have distinct mechanisms. The interaction of CTLA-4 and PD-1 is unclear. However, our data showed that blocking PD-1 somehow caused a significant reduction in CTLA-4 expression in Tregs. Understanding to what extent PD-1 and CTLA-4 use similar or distinct mechanisms to block T-cell activation will have important implications in the design of immunotherapies to modify allergic immune responses.

Costimulatory molecules and their interactions are pivotal in the activation and function of Tregs. Recently, Jen and colleagues (31) demonstrated that blocking CD45RB with a CD45RB antagonist resulted in a substantial increase in airway inflammation. However, the administration of a CD45RB agonist caused a significant decrease in airway inflammation and a substantial increase of CTLA-4 mRNA expression. These data suggest that the upregulation and/or cell surface expression of costimulatory molecules may involve a dependent or independent mechanism for T-cell activation and function. Further studies are needed to

TABLE 1. BALF CYTOKINES

Treatment Groups	Concentration of BALF Cytokines (pg/ml)			
	IL-4	IL-5	IL-10	IL-13
L25^{+}				
PBS	52.4 ± 4.73	31.8 ± 3.23	4.35 ± 1.32	1.83 ± 0.202
PBS^{AT+}	53.7 ± 2.03	20.1 ± 1.12	6.63 ± 0.957	5.16 ± 0.601
CRA^{AT+-}	315 ± 24.3†	756 ± 5.23†	107 ± 4.97*	86.3 ± 5.65†
CRA^{AT+}	78.3 ± 10.9†	74.3 ± 4.16†	354 ± 17.8†	3.13 ± 0.983‡
aPD-1^{ab} + CRA^{AT+}	633 ± 15.8†	806 ± 11.1†	62.7 ± 6.35*	73.8 + 3.64†
L25^{-}				
PBS	46.7 ± 9.28	39.4 ± 3.31	10.1 ± 1.31	0 ± 0
PBS^{AT+}	43.3 ± 13.6	23.2 ± 4.23	12.6 ± 1.48	0 ± 0
CRA^{AT+-}	645 ± 9.01†	614 ± 5.71‡	65.2 ± 3.83*	177 ± 11.3*
CRA^{AT+}	97.3 ± 13.8†	30.4 ± 1.71†	415 ± 16.4†	5.83 + 0.883†
aPD-1^{ab} + CRA^{AT+}	424 ± 20.6†	503 ± 2.89‡	158 ± 12.3*	208 ± 21.3
S25^{+}				
PBS	52.3 ± 5.04	0 ± 0	0 ± 0	16.4 ± 3.81
PBS^{AT+}	44.3 ± 4.70	4.23 ± 0.481	0 ± 0	1.67 ± 0.147
CRA^{AT+-}	282 ± 5.78‡	483 ± 7.62†	48.3 ± 3.17*	94.4 ± 3.51†
CRA^{AT+}	80.2 ± 5.46†	88.6 ± 2.91†	485 ± 29.7*	35.6 ± 9.27*
aPD-1^{ab} + **CRA^{AT+}**	515 ± 18.6†	500 ± 12.7†	342 ± 17.3*	114 ± 9.26†
S25^{-}				
PBS	36.2 ± 3.81	0 ± 0	19.5 ± 1.89	3.13 ± 1.51
PBS^{AT+}	56.7 ± 4.42	0 ± 0	23.3 ± 4.91	0 ± 0
CRA^{AT+-}	484 ± 10.3†	613 ± 30.4*	103 ± 10.4†	102 ± 10.1*
CRA^{AT+}	83.4 ± 13.5†	35.1 ± 3.05*	436 ± 19.3*	3.76 ± 0.963†
aPD-1^{ab} + CRA^{AT+}	384 ± 11.8†	597 ± 7.61†	92.6 ± 9.82†	208 ± 22.7*

Data are shown as mean ± SEM (n = 3 in each experimental group).
* $P < 0.01$.
† $P < 0.001$.

elucidate the role of costimulatory molecules in CD4^{+}CD25^{+} Tregs.

An alternative mechanism to explain the role of PD-1 expression by Tregs may involve the IL-2 receptor. Burchill and colleagues (32) demonstrated that IL-2Rβ knockout mice developed autoimmunity. However, these mice were rescued from disease progression after being reconstituted with CD4^{+} T cells expressing Foxp3, suggesting that Foxp3 expression is dependent on IL-2Rβ signaling. These investigators later showed that IL-2Rβ signaling was dependent on STAT5 activation for the development of Tregs (32). Recently, Franceschini and colleagues (33) demonstrated that blocking the PD-1/PD-L1 axis with a PD-1 antagonist correlated with a significant increase in phosphorylated STAT5, allowing STAT5 to translocate to the nucleus and bind to the IL-2 promoter, causing an inhibition of autocrine IL-2 secretion by Tregs. The inhibition of IL-2 prevented Treg proliferation, and allowed for the development of skewed T-cell ratios. These reports may support our finding that CD4^{+}CD25^{+} T cells isolated from the lungs of all groups that received an adoptive transfer of either NTregs or iTregs from either tissue type plus aPD-1^{ab} exhibited a significant decrease in mRNA transcripts of Foxp3, compared with CD4^{+}CD25^{+} T cells isolated from all groups of mice that received an adoptive transfer only.

The decreased expression of Foxp3 mRNA from CD4^{+}CD25^{+} T cells isolated from lungs of mice treated with aPD-1^{ab} was quantitatively similar to that in CRA-sensitized mice without adoptive transfer. These CD4^{+}CD25^{+} Tregs isolated from the lungs of aPD-1^{ab}–treated mice that were Foxp3-deficient lacked immunosuppressive ability, as demonstrated by their elevated AHR and severely remodeled airways. These data suggest that PD-L1/PD-1 and PD-L2/PD-1 axes are critical for Foxp3 expression, depending on the pathologic condition. Krupnick and colleagues showed that blocking PD-1 significantly reduced the expression of Foxp3 in vascular endothelial tissue, and prevented the conversion of CD4^{+}CD25^{-} T cells into CD4^{+}CD25^{+} T cells (34, 35). Both PD-1 and CTLA-4 appear to be crucial markers in the control of T-cell tolerance, and this action possibly occurs via Foxp3 expression. Wang and colleagues (36) demonstrated that PD-L1/PD1 signaling is necessary for the development of inducible CD4^{+} Tregs. In another study, CTLA-4 knockout mice exhibited similarities to scurfy mice, with an absence of NTregs and deficiency in Foxp3 expression (37). Polanczyk and colleagues (29) showed that PD-1 knockout mice retained normal levels of Foxp3 expression, but the Tregs isolated from these mice lacked the functional suppression. The expression of Foxp3 and its correlation with the expression of PD-1 and CTLA-4 are unclear. However, in the absence of either costimulatory molecule, Tregs appear to demonstrate a significant deficiency in the modulation of immune response. In addition, blocking PD-1 resulted in an increase in pulmonary eosinophilia and lymphocytosis. The increase of eosinophils in BALF from blocking PD-1 is unclear, but may be attributable to the fact that the ligands for PD-1 (PD-L1 and PD-L2) were unable to bind the receptor. The inhibition of PD-L2 induces an increase in pulmonary eosinophils (38, 39). In other disease models, anti–PD-L1 and anti–PD-L2 during the induction phase of EAE increased the onset of disease symptoms (16, 40). Our findings suggest that PD-1 and possibly CTLA-4 may play a role in the differential expression of Foxp3, but the molecular pathway merits further investigation.

Furthermore, the anti–PD-1 antagonist induced a significant increase in Th2 BALF cytokines, IL-4, IL-5, and IL-13. It seems likely that because PD-1 delivers a negative signal for CD4^{+} T-cell activation, blocking PD-1 induced a polarized Th2 cell response, which promoted the increase of Th2 cytokines seen in the BALF of mice that received aPD-1^{ab}. A similar phenomenon was reported by Wang and colleagues (39), i.e., blocking PD-1 in CD4^{+} T cells and stimulation with antigen induced a significant increase in the release of IL-5, IL-13, granulocyte/macrophage colony–stimulating factor, and IFN-γ *in vitro*. Cai and colleagues (41) showed an increase in showed an increase in Th2 cytokines when the PD-1/PD-L1 and PD-L2 axis was inhibited on naive and memory T cells, but more importantly on activated CD4+ T cells using myelin basic protein. Thus, our data correlate with other reports that the blockade of PD-1 causes an increase in T-cell activation, resulting in increased Th2 cytokine production. In addition, we found significantly increased concentrations of IFN-γ in the BALF of cockroach-sensitized and cockroach-challenged mice with adoptive transfer, compared with cockroach-sensitized and cockroach-challenged mice without adoptive transfer, and cockroach-sensitized mice with adoptive transfer plus aPD-1^{ab}. The increase in IFN-γ may constitute a secreted product from Tregs, or Th1-released IFN-γ may contribute to the development of Tregs. In a murine model of EAE, Wang and colleagues (36) showed that IFN-γ was required to convert naive CD4^{+}CD25^{-} T cells into CD4^{+}CD25^{+}Foxp3^{+} Tregs. The adoptive transfer of these converted Tregs into mice suppressed EAE and disease progression (39). Recently, Fang and colleagues (42) demonstrated that IFN-γ, produced from Th1-like adaptive Tregs, suppressed acute murine spotted fever rickettsiosis, an action that may be attributable to the expression of CTLA-4 and the secretion of IL-10. In our study, however, we do not know why IFN-γ concentrations decreased in cockroach-sensitized and cockroach-challenged mice with adoptive transfer plus aPD-1^{ab}. It is tempting to speculate that blocking PD-1 in the periphery could have inhibited the concentrations of IFN-γ required for the differentiation and/or function of inducible Tregs. This may account for the increase in AHR, airway inflammation, and decreased expression of Foxp3 in CD4^{+}CD25^{+} Tregs of mice treated with aPD-1^{ab}. However, this idea warrants further investigation.

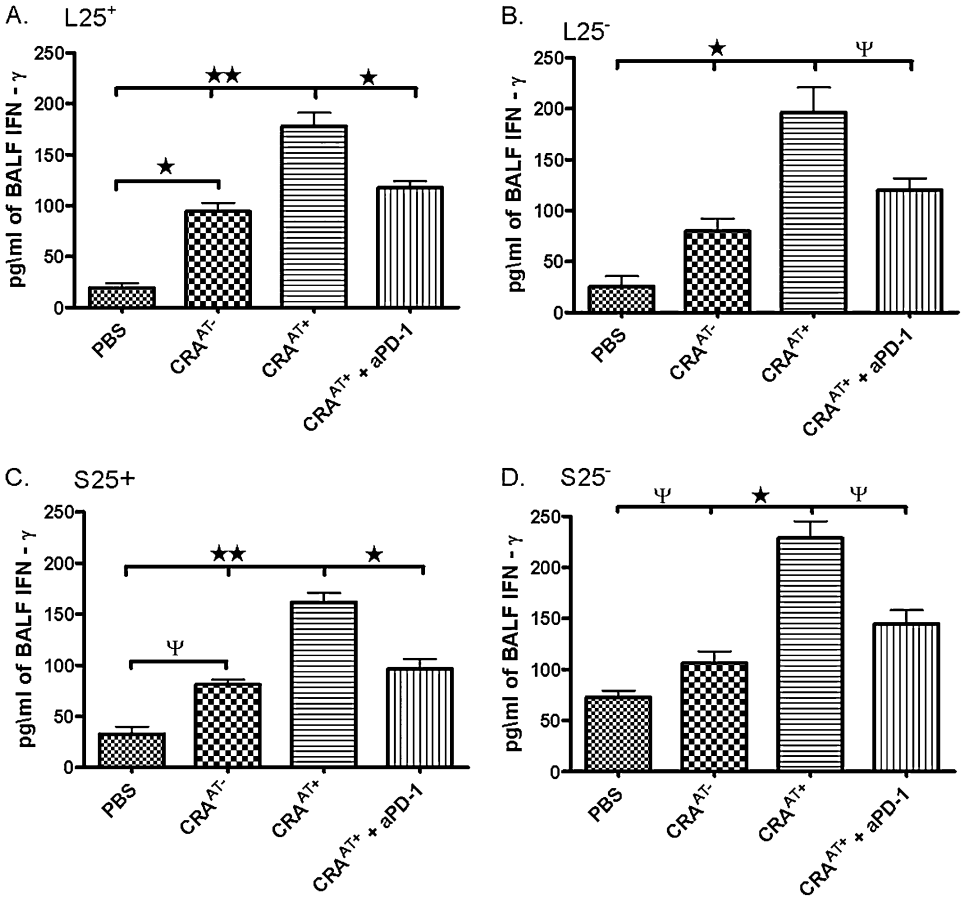

Figure 8. Concentrations of IFN-γ from BALF of cockroach-sensitized and cockroach-challenged mice. After final methacholine challenge, mice were killed and BALF was collected, and IFN-γ levels were analyzed using an ELISA Th1 and Th2 Ready-Set-Go Kit. Data are shown as mean ± SEM for three mice in each group. $^{\Psi}P < 0.05$, $^{*}P < 0.01$, $^{**}P < 0.001$.

It is interesting to observe the modest increase in IL-10 concentrations in CRA-sensitized and CRA-challenged mice in the absence of an adoptive transfer of Tregs, and also the high concentrations of IL-10 in the CRA-sensitized and CRA-challenged mice with adoptive transfer and the addition of aPD-1[ab]. This may suggest the presence of Th2 cells. We recently reported that $CD4^+CD25^+$ T cells isolated from the lungs of cockroach-sensitized and cockroach-challenged mice without adoptive transfer of Tregs showed a significant increase in the expression of GATA3 transcripts, i.e., the transcriptional factor of Th2 cells (24). Interleukin-10 was initially reported to be a secreted product of Th2 cells (43). Moreover, Th2 cells are also known to secrete their signature cytokines, including IL-4, IL-5, IL-9, and IL-13. However, the production of IL-10 by Th2 cells may involve a negative feedback loop to limit collateral tissue damage and the progression of immune pathology (44). On the other hand, the substantially high concentrations of IL-10 in cockroach-sensitized and cockroach-challenged mice adoptively transferred with Tregs could be indicative of the presence of Tregs, and specifically iTregs. This subset of Tregs is known to secrete copious amounts of IL-10 (45, 46). There are several potential explanations for the elevated levels of IL-10 in the cockroach-sensitized and cockroach-challenged mice plus adoptive transfer and anti–PD-1 antibody. These explanations contend that: (*1*) established AHR by cockroach sensitization may initially lead to a moderate increase of IL-10 concentrations by Th2 cells; (*2*) the adoptive transfer of Tregs may have also augmented these concentrations, because these cells are major producers of IL-10; or (*3*) after optimal binding was achieved by the anti–PD-1 antibody to Tregs and possibly other cell types, IL-10 production may have been decreased. In an anterior chamber-associated immune deviation model, Wang and colleagues (43) showed that $CD4^+PD\text{-}1^+$ T cells exhibited an enhanced expression of IL-10 compared with $CD4^+PD\text{-}1^-$ T cells. Therefore, blocking PD-1 may cause a decrease in IL-10 expression and secretion. However, this concept warrants further investigation, to explain the relationship between PD-1 and IL-10 release.

In conclusion, we found that the adoptive transfer of Tregs reversed AHR and airway inflammation. However, inhibiting PD-1 with an antagonist blocked the therapeutic properties of the adoptive transfer of Tregs. In addition, these data showed that blocking PD-1 substantially elevated Th2 cytokines, but significantly increased anti-inflammatory cytokine and IL-10, and dramatically decreased the expression of CTLA-4. Thus, increasing the expression and/or activity of PD-1 and perhaps their ligands, PD-L1 and PD-L2, could offer a target for better therapeutic approaches to allergic asthma.

Author Disclosure: None of the authors has a financial relationship with a commercial entity that has an interest in the subject of this manuscript.

References

1. Takeda M, Ito W, Tanabe M, Ueki S, Kato H, Kihara J, Tanigai T, Chiba T, Yamaguchi K, Kayaba H, *et al.* Allergic airway hyperresponsiveness, inflammation, and remodeling do not develop in phosphoinositide 3-kinase gamma-deficient mice. *J Allergy Clin Immunol* 2009;123:805–812.
2. Akbari O, Faul JL, Hoyte EG, Berry GJ, Wahlstrom J, Kronenberg M, DeKruyff RH, Umetsu DT. $CD4^+$ invariant T-cell-receptor$^+$ natural killer T cells in bronchial asthma. *N Engl J Med* 2006;354:1117–1129.
3. Riccioni G, Di Ilio C, D'Orazio N. Review: pharmacological treatment of airway remodeling: inhaled corticosteroids or antileukotrienes? *Ann Clin Lab Sci* 2004;34:138–142.
4. Barnes PJ. Th2 cytokines and asthma: an introduction. *Respir Res* 2001;2:64–65.

5. Larche M. Regulatory T cells in allergy and asthma. *Chest* 2007;132: 1007–1014.
6. Ono M, Yaguchi H, Ohkura N, Kitabayashi I, Nagamura Y, Nomura T, Miyachi Y, Tsukada T, Sakaguchi S. Foxp3 controls regulatory T-cell function by interacting with AML1/Runx1. *Nature* 2007;446:685–689.
7. Taylor A, Verhagen J, Akdis CA, Akdis M. T regulatory cells in allergy and health: a question of allergen specificity and balance. *Int Arch Allergy Immunol* 2004;135:73–82.
8. Joetham A, Takeda K, Taube C, Miyahara N, Matsubara S, Koya T, Rha YH, Dakhama A, Gelfand EW. Naturally occurring lung CD4(+)CD25(+) T cell regulation of airway allergic responses depends on IL-10 induction of TGF-beta. *J Immunol* 2007;178:1433–1442.
9. Encinas JA, Wicker LS, Peterson LB, Mukasa A, Teuscher C, Sobel R, Weiner HL, Seidman CE, Seidman JG, Kuchroo VK. QTL influencing autoimmune diabetes and encephalomyelitis map to a 0.15-cM region containing IL2. *Nat Genet* 1999;21:158–160.
10. Sakaguchi S. Naturally arising Foxp3-expressing $CD25^+CD4^+$ regulatory T cells in immunological tolerance to self and non-self. *Nat Immunol* 2005;6:345–352.
11. Sakaguchi S, Ono M, Setoguchi R, Yagi H, Hori S, Fehervari Z, Shimizu J, Takahashi T, Nomura T. $Foxp3^+$ $CD25^+$ $CD4^+$ natural regulatory T cells in dominant self-tolerance and autoimmune disease. *Immunol Rev* 2006;212:8–27.
12. Gazzola L, Tincati C, Gori A, Saresella M, Marventano I, Zanini F. FoxP3 mRNA expression in regulatory T cells from patients with tuberculosis. *Am J Respir Crit Care Med* 2006;174:356 (author reply 357).
13. Lopes JE, Torgerson TR, Schubert LA, Anover SD, Ocheltree EL, Ochs HD, Ziegler SF. Analysis of FOXP3 reveals multiple domains required for its function as a transcriptional repressor. *J Immunol* 2006;177:3133–3142.
14. McNeill A, Spittle E, Backstrom BT. Partial depletion of CD69low-expressing natural regulatory T cells with the anti-CD25 monoclonal antibody PC61. *Scand J Immunol* 2007;65:63–69.
15. Nishimura H, Honjo T. PD-1: an inhibitory immunoreceptor involved in peripheral tolerance. *Trends Immunol* 2001;22:265–268.
16. Butte MJ, Keir ME, Phamduy TB, Sharpe AH, Freeman GJ. Programmed death-1 ligand 1 interacts specifically with the B7-1 costimulatory molecule to inhibit T cell responses. *Immunity* 2007;27:111–122.
17. Fukushima A, Yamaguchi T, Azuma M, Yagita H, Ueno H. Involvement of programmed death-ligand 2 (PD-L2) in the development of experimental allergic conjunctivitis in mice. *Br J Ophthalmol* 2006;90: 1040–1045.
18. Chemnitz JM, Parry RV, Nichols KE, June CH, Riley JL. SHP-1 and SHP-2 associate with immunoreceptor tyrosine-based switch motif of programmed death 1 upon primary human T cell stimulation, but only receptor ligation prevents T cell activation. *J Immunol* 2004;173:945–954.
19. Corry DB, Grunig G, Hadeiba H, Kurup VP, Warnock ML, Sheppard D, Rennick DM, Locksley RM. Requirements for allergen-induced airway hyperreactivity in T and B cell-deficient mice. *Mol Med* 1998;4:344–355.
20. Okazaki T, Honjo T. The PD-1-PD-L pathway in immunological tolerance. *Trends Immunol* 2006;27:195–201.
21. Freeman GJ, Long AJ, Iwai Y, Bourque K, Chernova T, Nishimura H, Fitz LJ, Malenkovich N, Okazaki T, Byrne MC, *et al.* Engagement of the PD-1 immunoinhibitory receptor by a novel B7 family member leads to negative regulation of lymphocyte activation. *J Exp Med* 2000;192:1027–1034.
22. Hong J, Li N, Zhang X, Zheng B, Zhang JZ. Induction of $CD4^+CD25^+$ regulatory T cells by copolymer-I through activation of transcription factor Foxp3. *Proc Natl Acad Sci USA* 2005;102:6449–6454.
23. Yadav D, Sarvetnick N. Costimulation and pancreatic autoimmunity: the PD-1/PD-L conundrum. *Rev Diabet Stud* 2006;3:6–10.
24. McGee HS, Agrawal DK. Naturally occurring and inducible T-regulatory cells modulating immune response in allergic asthma. *Am J Respir Crit Care Med* 2009, 180:211–225.
25. McGee HS, Edwan JH, Agrawal DK. Flt3-L increases $CD4^+CD25^+Foxp3^+ICOS^+$ cells in the lung of cockroach-sensitized and challenged mice. *Am J Respir Cell Mol Biol* 2009, 42:331–340.
26. Agata Y, Kawasaki A, Nishimura H, Ishida Y, Tsubata T, Yagita H, Honjo T. Expression of the PD-1 antigen on the surface of stimulated mouse T and B lymphocytes. *Int Immunol* 1996;8:765–772.
27. Ansari MJ, Salama AD, Chitnis T, Smith RN, Yagita H, Akiba H, Yamazaki T, Azuma M, Iwai H, Khoury SJ, *et al.* The programmed death-1 (PD-1) pathway regulates autoimmune diabetes in nonobese diabetic (NOD) mice. *J Exp Med* 2003;198:63–69.
28. Nishimura H, Minato N, Nakano T, Honjo T. Immunological studies on PD-1 deficient mice: implication of PD-1 as a negative regulator for B cell responses. *Int Immunol* 1998;10:1563–1572.
29. Polanczyk MJ, Hopke C, Vandenbark AA, Offner H. Treg suppressive activity involves estrogen-dependent expression of programmed death-1 (PD-1). *Int Immunol* 2007;19:337–343.
30. Parry RV, Chemnitz JM, Frauwirth KA, Lanfranco AR, Braunstein I, Kobayashi SV, Linsley PS, Thompson CB, Riley JL. CTLA-4 and PD-1 receptors inhibit T-cell activation by distinct mechanisms. *Mol Cell Biol* 2005;25:9543–9553.
31. Jen KY, Campo M, He H, Makani SS, Velasco G, Rothstein DM, Perkins DL, Finn PW. CD45RB ligation inhibits allergic pulmonary inflammation by inducing CTLA4 transcription. *J Immunol* 2007;179: 4212–4218.
32. Burchill MA, Yang J, Vogtenhuber C, Blazar BR, Farrar MA. IL-2 receptor beta-dependent STAT5 activation is required for the development of $Foxp3^+$ regulatory T cells. *J Immunol* 2007;178:280–290.
33. Franceschini D, Paroli M, Francavilla V, Videtta M, Morrone S, Labbadia G, Cerino A, Mondelli MU, Barnaba V. PD-L1 negatively regulates $CD4^+CD25^+Foxp3^+$ Tregs by limiting STAT-5 phosphorylation in patients chronically infected with HCV. *J Clin Invest* 2009;119:551–564.
34. Zhou H, Zhang L, Tong L, Cai M, Guo H, Yang C, Shi B, Chen ZK. Expression of neuropilin-1 in kidney graft biopsies: what is the significance? *Transplant Proc* 2007;39:81–83.
35. Krupnick AS, Gelman AE, Barchet W, Richardson S, Kreisel FH, Turka LA, Colonna M, Patterson GA, Kreisel D. Murine vascular endothelium activates and induces the generation of allogeneic $CD4^+25^+Foxp3^+$ regulatory T cells. *J Immunol* 2005;175:6265–6270.
36. Wang L, Pino-Lagos K, de Vries VC, Guleria I, Sayegh MH, Noelle RJ. Programmed death 1 ligand signaling regulates the generation of adaptive $Foxp3^+CD4^+$ regulatory T cells. *Proc Natl Acad Sci USA* 2008;105:9331–9336.
37. Wing K, Fehervari Z, Sakaguchi S. Emerging possibilities in the development and function of regulatory T cells. *Int Immunol* 2006;18:991–1000.
38. Matsumoto K, Inoue H, Nakano T, Tsuda M, Yoshiura Y, Fukuyama S, Tsushima F, Hoshino T, Aizawa H, Akiba H, *et al.* B7-DC regulates asthmatic response by an IFN-gamma-dependent mechanism. *J Immunol* 2004;172:2530–2541.
39. Wang Z, Hong J, Sun W, Xu G, Li N, Chen X, Liu A, Xu L, Sun B, Zhang JZ. Role of IFN-gamma in induction of Foxp3 and conversion of $CD4^+$ $CD25^-$ T cells to $CD4^+$ Tregs. *J Clin Invest* 2006;116:2434–2441.
40. Chen Z, Laurence A, Kanno Y, Pacher-Zavisin M, Zhu BM, Tato C, Yoshimura A, Hennighausen L, O'Shea JJ. Selective regulatory function of Socs3 in the formation of IL-17-secreting T cells. *Proc Natl Acad Sci USA* 2006;103:8137–8142.
41. Cai G, Karni A, Oliveira EM, Weiner HL, Hafler DA, Freeman GJ. PD-1 ligands, negative regulators for activation of naive, memory, and recently activated human $CD4^+$ T cells. *Cell Immunol* 2004;230:89–98.
42. Fang R, Ismail N, Shelite T, Walker DH. $CD4^+$ $CD25^+$ $Foxp3^-$ T-regulatory cells produce both gamma interferon and interleukin-10 during acute severe murine spotted fever rickettsiosis. *Infect Immun* 2009;77:3838–3849.
43. Wang ZY, Sato H, Kusam S, Sehra S, Toney LM, Dent AL. Regulation of IL-10 gene expression in Th2 cells by Jun proteins. *J Immunol* 2005;174:2098–2105.
44. O'Garra A, Vieira PT. (H)1 cells control themselves by producing interleukin-10. *Nat Rev Immunol* 2007;7:425–428.
45. Nandakumar S, Miller CW, Kumaraguru U. T regulatory cells: an overview and intervention techniques to modulate allergy outcome. *Clin Mol Allergy* 2009;7:5.
46. Wu K, Bi Y, Sun K, Wang C. IL-10-producing type 1 regulatory T cells and allergy. *Cell Mol Immunol* 2007;4:269–275.

Reproduced with permission of the copyright owner. Further reproduction prohibited without permission.